Bioorganic & Medicinal Chemistry 16 (2008) 8535–8545

Contents lists available at ScienceDirect

Bioorganic & Medicinal Chemistry

journal homepage: www.elsevier.com/locate/bmc

Theoretical analysis of the electronic properties of the sex pheromone and its analogue derivatives in the female processionary moth *Thaumetopoea pytiocampa*

Ester R. Chamorro [b], Alfredo F. Sequeira [b], M. Fernanda Zalazar [a,b], Nélida M. Peruchena [a,b,*]

[a] Laboratorio de Estructura Molecular y Propiedades, Area de Química Física, Depto. Química, Fac. Ciencias Exactas, Nat. y Agrim., UNNE, Avda. Libertad 5460, (3400) Corrientes, Argentina
[b] QUIMOBI, Facultad Regional Resistencia, Universidad Tecnológica Nacional, French 414 Resistencia, Chaco, Argentina

ARTICLE INFO

Article history:
Received 20 June 2008
Revised 28 July 2008
Accepted 4 August 2008
Available online 7 August 2008

Keywords:
Charge density
Laplacian
Molecular electrostatic potential
Sex pheromone
.

ABSTRACT

In the present work, the distribution of the electronic charge density of the natural sex pheromone, the (*Z*)-13-hexadecen-11-ynyl acetate, in the female processionary moth, *Thaumetopoea pytiocampa,* and its nine analogue derivatives was studied within the framework of the Density Functional Theory and the Atoms in Molecules (AIM) Theory at B3LYP/6-31G* //B3LYP/6-31++G** level. Additionally, molecular electrostatic potential (MEP) maps of the previously mentioned compounds were computed and compared. Furthermore, the substitution of hydrogen atoms from the methyl group in the acetate group by electron withdrawing substituents (i.e., halogen atoms) as well as the replacement effect of hydrogen by electron donor substituents (+I effect) as methyl group, were explored. The key feature of the topological distribution of the charge density in analogue compounds, such as the variations of the topological properties encountered in the region formed by neighbouring atoms from the substitution site were presented and discussed. Using topological parameters, such as electronic charge density, Laplacian, kinetic energy density, and potential energy density evaluated at bond critical points (BCP), we provide here a detailed analysis of the nature of the chemical bonding of these molecules. In addition, the atomic properties (population, charge, energy, volume, and dipole moment) were determined on selected atoms. These properties were analyzed at the substitution site (with respect to the natural sex pheromone) and related to the biological activity and to the possible binding site with the pheromone binding protein, (PBP). Moreover, the Laplacian function of the electronic density was used to locate electrophilic regions susceptible to be attacked (by deficient electron atoms or donor hydrogen).

Our results indicate that the change in the atomic properties, such as electronic population and atomic volume, are sensitive indicators of the loss of the biological activity in the analogues studied here. The crucial interaction between the acetate group of the natural sex pheromone and the PBP is most likely to be a hydrogen bonding and the substitution of hydrogen atoms by electronegative atoms in the pheromone molecule reduces the hydrogen acceptor capacity. This situation is mirrored by the diminish of the electronic population on carbon and oxygen atoms at the carbonylic group in the halo-acetate group. Additionally, the modified acetate group (with electronegative atoms) shows new charge concentration critical points or regions of concentration of charge density in which an electrophilic attack can also occur. Finally, the use of the topological analysis based in the charge density distribution and its Laplacian function, in conjunction with MEP maps provides valuable information about the steric volume and electronic requirement of the sex pheromone for binding to the PBP.

© 2008 Elsevier Ltd. All rights reserved.

1. Introduction

The specificity of insects' chemical language is fascinating and it is, often, the only means insects have for finding each other. In these last decades, the researchers have discovered the code for the pheromone communication of more than 1,600 insects. In addition, the insect behavior can be controlled by simple odor compounds or by blend of several components of the sex pheromone.[1]

Intensive activity is encountered in the study of how insects produce pheromones, how they trigger a response, and what influences that response. For example, researchers are beginning to uncover the hormones that trigger pheromone production as well as the binding proteins that bring the pheromones to their receptors.[2]

* Corresponding author. Tel.: +54 3783 457996; fax: +54 3783 473930.
E-mail address: peruchen@exa.unne.edu.ar (N.M. Peruchena).

0968-0896/$ - see front matter © 2008 Elsevier Ltd. All rights reserved.
doi:10.1016/j.bmc.2008.08.008

Other investigators also, are discovering the neurological pathways that the pheromones stimulate in a responding insect,[3] and the enzymes[4] the insects use to break down the pheromone so as to shut off its signaling.

This fascinating field of research should lead to the design of new molecules that affect an insect's response to pheromones, as well as better ways to use pheromones or other compounds or analogues to manage insect pests.[5] Currently, the interest is centered in expanding the successful use of pheromones in pest management. Considering that the insects have become increasingly resistant to conventional insecticides, and the fact that people became highly alert to the adverse effects of insecticides, research in the pheromone field is most necessary.

Lepidoptere pheromones are small organic molecules (10–20 non-hydrogen atoms), with low molecular weight. They have a hydrocarbonated chain of 10–16 carbon atoms, they are usually hydrophobic and volatile, and they, also, possess a polar group (acetate, or hydroxyl group). Interestingly enough, and even though they are simple molecules, they possess a very high specificity to activate the biological response.[6] Considering their chemical structure, the replacement of a hydrogen atom in the natural compound, for more electronegative atoms or group of atoms such as F, Cl, Br, CF_3, OH, etc., is used in the design of analogue molecules with synergistic effects similar to that of the natural compound. This constitutes a habitual practice in the design of chemotherapeutic compounds.[7]

In previous works, Camps et al. had fully characterized the sex pheromone of the pine processionary moth *Thaumetopoea pytiocampa*, *TP*, an important pest of pines. The structure of this pheromone has a long hydrocarbonated chain, a conjugated enyne group (—C≡C—C=C—) and an acetate group. The enyne group is a distinctive characteristic of the *TP* pheromone, and constitutes a unique feature in the pheromone field. In relation to this, several derivatives of the (*Z*)-13-hexadecen-11-ynyl acetate, with modification in the polar group (acetate group) have been synthesized by Camps et al.[8,9] The effect of the biological activity of these molecules have been determined in his laboratory through the response against a stimuli of the antennal receptors to vapours, (by electroantennogram);[10] and by the recording of the erratic flight of males treated with the analogue, in a wind tunnel.[11] Even though there are many structural similarities between the analogues and the natural sex pheromone in *TP*, the fluorinated derivatives can show a strong reduction of the biological activity and, in several cases, inhibitory effects.[12]

In general, it is accepted that the fluorine atom closely mimics the steric volume of the hydrogen atom. In contrast, the strong electronegativity of this halogen induces fluorinated compounds to a different behavior.[13a,13b]

The carrier protein responsible for the transport of the pheromone to the receptor through the lymph is the pheromone binding protein (PBP).[14] The PBP is present only in male sensillae and has showed some specificity as pheromone ligand with respect to other analogues. Some analogues (for example, the trifluoromethyl ketones (TFMKs)) can cause a disruption in the response compared to the natural sex pheromone.[12,15]

It is known that the TFMKs are potent inhibitors of a number of serine esterases[12,16] and proteases, such as acetylcholinesterase, chymotrypsin or human liver carboxylesterases.[17] In insect, these analogues reversibly inhibit the antennal esterases responsible for the catabolism of pheromone molecules in male olfactory tissues.[18] The electronic characteristic, possible conformations and chemical features of the natural sex pheromone analogues remain poorly known and only a few works can be found about them to date.

The knowledge of physicochemical properties and reactions sites of natural pheromone analogue compounds can provide a deeper insight of their possible mechanism of action. In consequence, theoretical studies of the natural sex pheromone and its analogues may help in the design of semi-chemical compounds with distinctive effects. Considering this, the electrostatic potential has been extensively used for interpreting and predicting the reactive behaviour of a wide variety of chemical systems.[19] They have been used in both, electrophilic and nucleophilic reactions. However, it has not been yet possible to determine accurately the sites for nucleophilic attack.[20] The reason to this is that the zones of positive potential are not necessarily expressing affinity for nucleophiles. In addition, molecular electrostatic potentials (MEPs) are well suited for analyzing processes based on the 'recognition' of one molecule by another, as in drug-receptor and enzyme-substrate interaction, because it is through their potentials that the two species first 'see' each other. In other words, it is through this potential that a molecule is first 'seen' or 'felt' by another approaching chemical species.[21,22] In the same way, when a ligand comes near to a receptor what they perceive are concentrations (CC) and depletions (CD) of the electronic density. These CCs and DCs in the valence shell of the atoms of a molecule can be quantitated and rigorously determined by the Laplacian of the charge density.[23]

In consequence, and even though the electrostatic potential (EP) has emerged as a useful analytical tool in the study of molecular reactivity, the electronic charge density is a more powerful property.[24] Electronic charge density is a real physical property that can be determined experimentally[25] by diffraction or by computational methods, using the rigorous principles of the quantum mechanics.[24] The theory of Atoms in Molecules (AIM), developed by Bader[26,27] is a key tool in the study of the electronic charge density. It is a simple, rigorous and elegant way of defining atoms, bonds, chemical structures and structural changes. Via topological analysis using AIM, a chemical structure may be unambiguously assigned to a molecule by determining the number and kind of critical points in its electronic charge distribution.

The local concentration and local depletion of electron charge density allow us to determine whether the nucleophile or electrophile can be attracted.[26] Considering this, the complementary binding of the ligand and its receptor is based on a stereo electronic recognition. Since no significant structural differences exist between the natural sex pheromone and selected analogues, it will be interesting to perform a deeper electronic study in these types of compounds.

In the present work, we report a computational study of the natural sex pheromone of the *T. pytiocampa* (**1**) and its analogue derivatives which were obtained by substitutions in the methyl group at the acetate function of the pheromone molecule (—OCO-R with R = —H (**2**) —CH_2CH_3 (**3**); —CH_2F (**4**); —CH_2Cl (**5**); —CHF_2 (**6**); —$CHCl_2$ (**7**); —CF_3 (**8**); —CCl_3 (**9**) and the analogue derivative (**10**), where the acetate group has been substituted by a hydroxyl group. We also provide a detailed analysis of the nature of the chemical bonding of these molecules, as well as the atomic properties and the possible attack site by PBP. In addition, we attempt to gain an insight about the relative contribution of the substituents to the ligand-receptor binding and relate them to the changes observed in the biological activity.

Finally, the determination of the bond critical points, BCPs, in the natural sex pheromone (**1**) and its analogues (compounds **2**–**10**), and the evaluation of their different topological parameters, allowed us to visualize the changes (depending on the nature of the substituent atom and the localization of the substitution in the skeleton pheromone), that operate on the distribution of the electronic density.

Currently, there are no systematic studies of the density distributions of these compounds that are highly specific in activating the process of communication among individuals of the same species.

2. Computational details

Starting at the minimal energy conformation of the sex pheromone, the (*Z*)-13-hexadecen-11-ynyl acetate, **1**, the geometries of all analogues obtained by substitution in the methyl group at the acetate function in the pheromone molecule (**2**–**9**) and the analogue derivative (**10**), where the acetate group has been substituted by hydroxyl group, were fully optimized (Scheme 1). Calculations at the Becke3 Lee–Yang–Parr (B3LYP) level[28] with the 6-31G* basis set were performed with the Gaussian03 suite program.[29] Geometrical variables were optimized using the Berny's analytical gradient method.[30] All stationary points were characterized as minimal energetic by calculating the Hessian matrix. The initial electronic study of the compounds was performed using molecular electrostatic potential. MEPs have been shown to provide reliable information both, on the interaction sites of the molecules with point charges, and on the comparative reactivities of these sites.[19] MEPs were obtained at the same computational level used for optimization. For visualization, the Molekel program (version 4.3) was used.[31] The electrostatic potential isosurface was calculated at B3LYP/6-31++G** level. Topological analysis of the electron charge density was performed using the AIMPAC[32] program. The Aim2000 program[33] was used to display molecular graphs and Laplacian critical points. The evaluation of the atomic properties was performed using the PROAIM[34] program with electron density obtained at B3LYP/6-31++G** level.

3. Results and discussion

As we mentioned before, the search for new, more stable, with pest controlling potential compounds and with pheromone-like activities in insects is encouraged in the computational field as well as in experimental field of syntheses.

Structural descriptors or parameters, such as bond distances or bond angles, hold little chemical information. However, if geometrical as well as electronic descriptors, (based on the molecular electronic density) are used for characterization of these bonds, then we should be able to extract (within the rigorous field of quantum mechanics), a maximum of chemical information.[35]

The —COO-R and —C≡C—C(H)═C(H)— moieties are important structural features in the natural sex pheromone in the context of its biological activities. In order to identify other structural and electronic features involved in the sex pheromone activity, we were able to test a set of closely related compounds presenting a modified —COO-R moiety. The substitution of an atom by another atom implicates many structural and electronic changes. In this section of our work we evaluated the molecular size and electronic properties of the studied compounds with the intention of understanding their role in the potential interactions with the pheromone binding protein. In order to compare the properties of the sex pheromone and its analogues at a same time, a tri-dimensional molecular electrostatic potential maps at the van der Waals contact surface, representing electrostatic potentials superimposed onto a surface of constant electron charge density (0.001 e/au.^{3}), are shown in Figure 1.

The coloring area in the graph represents the electrostatic potential, $V(r)$. As it is well known, the electrostatic potential is, by definition, the energy of interaction of a positively charge point with the nuclei and the electrons of a molecule. The electrostatic potential provides a representative measurement of the overall molecular charge distribution. The color code of this MEP maps is in the range of −0.0455 au. (deepest red) to +0.0235 au. (deepest blue) in all compounds, where red indicates the strongest attraction and blue indicates the strongest repulsion. Regions of negative $V(r)$ are usually associated with the lone pair of electronegative atoms and the π electrons of the unsaturated hydrocarbons.

The MEPs show an overall similarity for all studied derivatives, including the alcohol, compound **10**. All compounds display the higher negative potential at two extreme regions: (a) at the oxygen, fluorine and chlorine atoms in the acetate and acetate modified moieties, and (b) at the double and triple conjugated bond regions.

The elimination of the acetate group in compound **1** (the natural sex pheromone) and maintenance of one of the oxygen atoms leads to compound **10** the (*Z*)-13-hexadecen-11-yn-1-ol with no relevant changes in the concentration of the electronic density in the oxygen atom with respect to the natural sex pheromone.

More detailed information about the potential sites of the interactions can be obtained from the isopotential surface at −0.0125 au. in the different sex pheromone analogues. As stated before, Figure 2 shows the negative isopotential surfaces localized at the two ends of the molecule. We believe that an intermediate level of internal charge separation is required in the natural sex pheromone and its analogues so that they can be carried by the pheromone binding protein. This previous assertion fits in well considering that, and because of their hydrocarbonated chain, pheromones are lipid soluble compounds. Pheromones also possess a polar group (acetate or alcohol) as part of their chemical structure, indicating that some degree of hydrophilicity is, as well, necessary for its biological activity. The pheromone binding protein, apparently, operates through weak, non covalent and reversible interactions with certain sites of the sex pheromone pattern.

As we expected, analogues **2** and **3** showed general similarity to the natural sex pheromone. However, in analogues **4** to **9**, where the halo-acetate group possess mono, di and tri-halogenated groups, the isopotential surface displayed a higher area or region of negative potential compared to the natural sex pheromone (where the area in **4** < **6** < **8** and **5** < **7** < **9**). For example, in compound **6**, the negative potential wraps the fluorine and oxygen

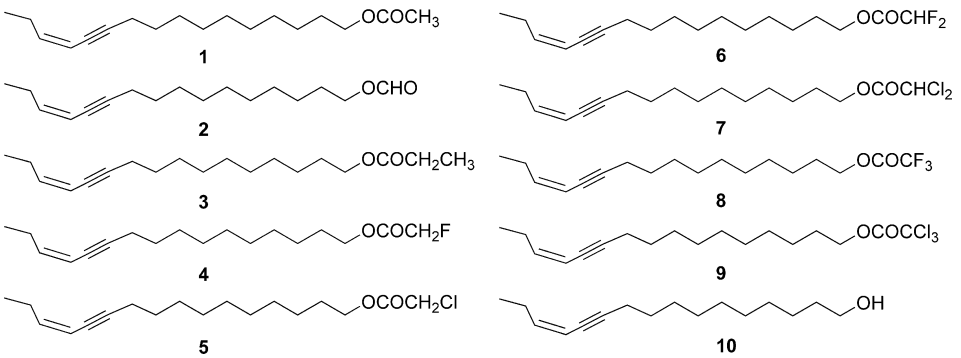

Scheme 1. Schematic representation of the (*Z*)-13-hexadecen-11-ynyl acetate and its analogs, compounds **1**–**10**.

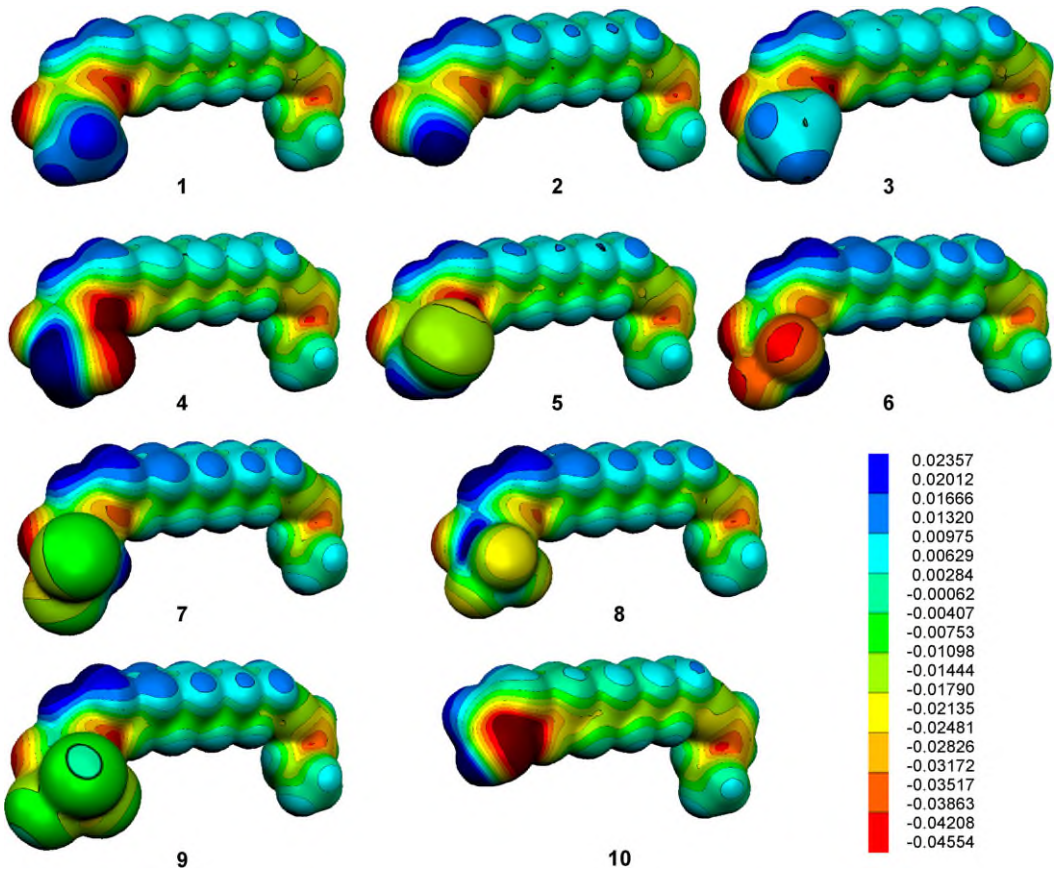

Figure 1. Molecular electronic potential maps onto a van der Waals surface (isodensity 0.001 e/au^3) for compounds **1**–**10**. The color-coded is shown at the right (in the range of –0.04557 au. (deepest red) to +0.02354 au. (deepest blue)).

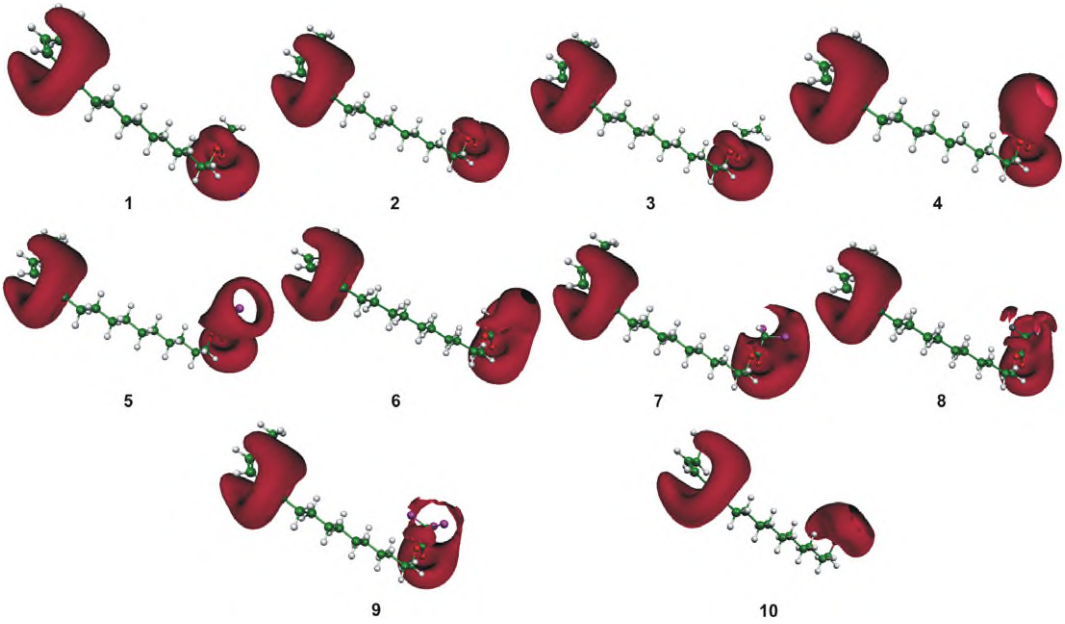

Figure 2. Electrostatic isopotential surface, ($V_{(r)} = -0.0125$ au.), in compounds **1**–**10** showing which sites are able to interaction with proton-donor reactants. Note in all cases the presence of two negative electrostatic potential regions corresponding to enyne group and acetate/modified acetate groups.

atoms in a continuum envelope. Similar results were observed in chlorinated compounds. In summary, the results obtained by isopotential surface are indicative of an increase of the attractive region upon the molecular surface in halogenated analogues.

3.1. Topology of the charge density

3.1.1. Local properties

Because the use of topological concepts is well documented in the standard literature, here, we only presented the essential theoretical information that is needed for the discussion of the numerical and graphical results. Considering that the atom that substitutes the hydrogen of the methyl group in the acetate moiety shares with the bounded carbon atom three topological elements related to each other (a point, a line and a surface), it is evident that the three elements will be modified by that substitution. In consequence, the exploration of topological properties related with these three topological elements is a matter of interest in the present work.

As it is well known, the critical point in the charge density topology that is found between two chemically bonded nuclei constitutes the first basic element: the bond critical point, BCP. From these BCP, two unique trajectories of gradient vectors of electronic density, $\nabla\rho_{(r)}$, originate at that point and terminate at each of the neighbouring nuclei. These trajectories define a line along which the density is a maximum with respect to any neighbouring line. This line is termed a bond path, BP, and constitutes the second element. Atoms so linked are bonded to one another and share a common interatomic surface, this constitutes the third element. Additionally, the set of trajectories that terminate at a BCP define the interatomic surface (IAS) that separates the atomic basins of the neighbouring atoms. Any IAS is such that it is a zero flux surface for $\nabla\rho_{(r)}$ and its significance in relation to the atomic properties will be discussed later.

We first, began with a brief description of the bonding topology in several representatives bonds in the natural sex pheromone and its analogues. All the BCPs were encountered from topological analysis of the electronic density and characterized by a set of local properties. Calculated properties at the BCP were labelled with the subscript 'b' throughout the work.

Figure 3 shows the molecular graph of the natural sex pheromone, (compound **1**). The BCPs are indicated in small circles and the BPs in bold lines. The big circles correspond to attractors attributed to positions of the nuclei.

Table 1 reports the calculated local topological properties in the natural sex pheromone: the electron densities (ρ_b), the Laplacian ($\nabla^2\rho_b$), the ellipticity (ε) and its three curvatures (λ_{1-3}), and the relationship between the perpendicular and parallel curvatures ($|\lambda_1|/\lambda_3$). The energetic relationship between the local kinetic energy density and the local potential energy density, $|V_b|/G_b$; the kinetic energy density by charge unit, G_b/ρ_b, and the total energy density, $E_{e(b)}$ are also included. However, only a few representative bonds (i.e., C—H, C—C, and C—O) at the acetate region are presented and analysed in this section. (Information related to local topological properties at other BCPs can be solicited to the authors).

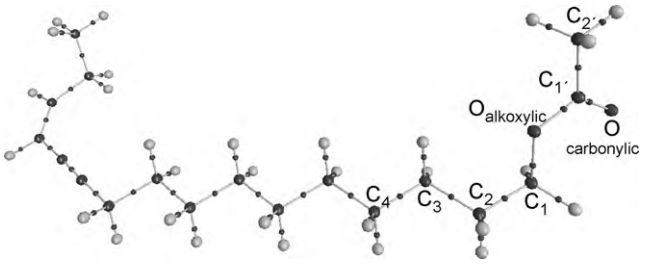

Figure 3. Molecular graph for natural sex pheromone. Big circles correspond to attractors attributed to nuclei, lines connecting the nuclei are the bond paths and the small circles on them are the BCP.

Figure 4a–c shows in a vertical bar chart the values of the charge density, Laplacian and $E_{e(b)}$ at the BCP in three different C—O bonds in all compound. In this figure the values of the natural sex pheromone, previously reported in Table 1, are expressed as a control group in order to have a comparative relation with the analogue compounds.

Usually, in shared interactions the charge density is accumulated between two bonded nuclei and the Laplacian is of the same order of magnitude as the charge density. Habitually, in these interactions the Laplacian takes negative values, even though a positive Laplacian may occur for polar covalent bonds, (e.g., the double bonds between C and O, and the single bonds between C and F or C and Cl). In accordance with the previous statement, it can be seen that the carbonylic C—O bonds are either shared or covalent interactions. They have the higher values of charge density at the BCP, ($\rho_b > 0.40$ au.) and a small Laplacian, $\nabla^2\rho_b$, that is > 0. Consequently, the charge density of the alkoxylic C—O bond is lower than the adjacent carbonylic bond (ρ_b is around 0.30 au.) and higher than the other alkoxylic C_1—O bond ($\rho_b < 0.25$ au.). Likely, the Laplacian values are negative on these bonds, being of major magnitude in the $C_{1'}$—O bonds.

Following in Table 1, more information about the C—O bonds is been provided. Once the parameters obtained from the BCP on the carbonylic and the alkoxylic bonds are analyzed, two different characteristic about the Laplacian values can be clearly seen. Table 1 and Figure 4 show that $\nabla^2\rho_b$ values are small and positive in all carbonylic bonds and negative in all alkoxylic bonds. In spite of this, the total energy density values are negative in both bond types.

In previous works, Cremer et al.[36] have used the total energy density, $E_{e(b)}$, to complement the Laplacian in the analysis of bond types. $E_{e(b)}$ is given by $(V_b + G_b)$, and its value at a BCP is negative for 'shared interactions', and positive for 'closed-shell interactions' as it is shown in Table 1. Unlike the Laplacian value, that is determined by the local virial expression[26] (and it is analyzed later on), the value of $E_{e(b)}$ is determined by the energy density itself and therefore is negative for all interactions, that results in an accumulation of electronic charge density at the BCP (see Table 1).

The alkoxylic C-O (C_1—O and $C_{1'}$—O) bonds show covalent bond characteristics with electronic charge density values around 0.30–0.32 au. for $C_{1'}$—O bonds and 0.22–0.23 au. for C_1—O bonds and negative Laplacian values $\nabla^2\rho_b = -0.5069$ in the natural sex pheromone that diminish to −0.463 au. in the trifluorinated compound **8** in $C_{1'}$—O bonds and similarly −0.3598 au. that diminished to −0.287 au. in C_1—O bonds.

In relation to the curvatures values at the BCP in carbonylic bonds, a positive Laplacian at BCP denotes that the perpendicular contraction of charge toward the AIL ($\lambda_{1,2}$) is less significant than the longitudinal depletion of charge away from the BCP, toward the nuclei (λ_3). In addition, the curvatures of the charge density are extensively large ($\lambda_1 = -1.1195$, $\lambda_2 = -1.0122$ and $\lambda_3 = +2.2220$ in compound **1** and assumes similar values in the other compounds). The ellipticity values reveal a double bond character, suitable to carbonylic C—O bonds.

As was previously expressed, the curvatures at BCP are higher in carbonylic than in alkoxylic bonds. Moreover, the curvature value in the direction of the bond in carbonylic bond is double than in the perpendicular direction (Fig. 5); resulting in $|\lambda_1|/\lambda_3$ values near to 0.50 in all studied compounds. The $|\lambda_1|/\lambda_3$ relationship is higher in alkoxylic than carbonylic bonds (See Table 1).

Furthermore, the relationship $|V_b|/G_b$ in carbonylic C—O bonds is slightly lower than 2 and, in consequence; the Laplacian values are small and positive. In contrast, this relationship in alkoxylic C—O bonds is slightly higher than 2, resulting in negative Laplacian values. In consequence, the total energy density is negative in both situations, as was expressed above.

Table 1
Local topological properties (in au.) of the electronic charge density distribution calculated at the position of the bond critical points of selected bond paths for species 1[a]

Bond	ρ_b	$\nabla^2\rho_b$	ε	λ_1	λ_2	λ_3	$\lvert\lambda_1\rvert/\lambda_3$	$\lvert V_b\rvert/G_b$	G_b/ρ_b	$E_{e(b)}$
$C_{1'}$-$O_{(carbonylic)}$	0.4146	0.0903	0.106	−1.1195	−1.0122	2.2220	0.5038	1.9695	1.7836	−0.7169
$C_{1'}$-$O_{(alkoxylic)}$	0.2999	−0.5069	0.001	−0.6459	−0.6451	0.7841	0.8237	2.3698	1.1427	−0.4694
C_1-$O_{(alkoxylic)}$	0.2342	−0.3598	0.017	−0.3972	−0.3906	0.4281	0.9279	2.3945	0.9736	−0.3179
$C_{1'}$-$C_{2'}$	0.2597	−0.6488	0.069	−0.5201	−0.4867	0.3580	1.4528	4.7262	0.2291	−0.2217
$C_{2'}$-H	0.2752	−0.9450	0.010	−0.7130	−0.7061	0.4740	1.5040	7.3669	0.1600	−0.2803
$C_{2'}$-H	0.2750	−0.9437	0.010	−0.7122	−0.7053	0.4738	1.5032	7.3503	0.1603	−0.2800
$C_{2'}$-H	0.2809	−0.9925	0.009	−0.7395	−0.7328	0.4798	1.5413	7.9089	0.1495	−0.2901
C_1-C_2	0.2520	−0.5980	0.043	−0.4877	−0.4676	0.3573	1.3648	4.6337	0.2252	−0.2063
C_2-C_3	0.2427	−0.5479	0.008	−0.4486	−0.4452	0.3459	1.2971	4.4633	0.2292	−0.1926
C_3-C_4	0.2436	−0.5523	0.011	−0.4525	−0.4476	0.3479	1.3008	4.4874	0.2279	−0.1936

[a] See text and Figure 1 for an explanation of symbols and identification of atoms.

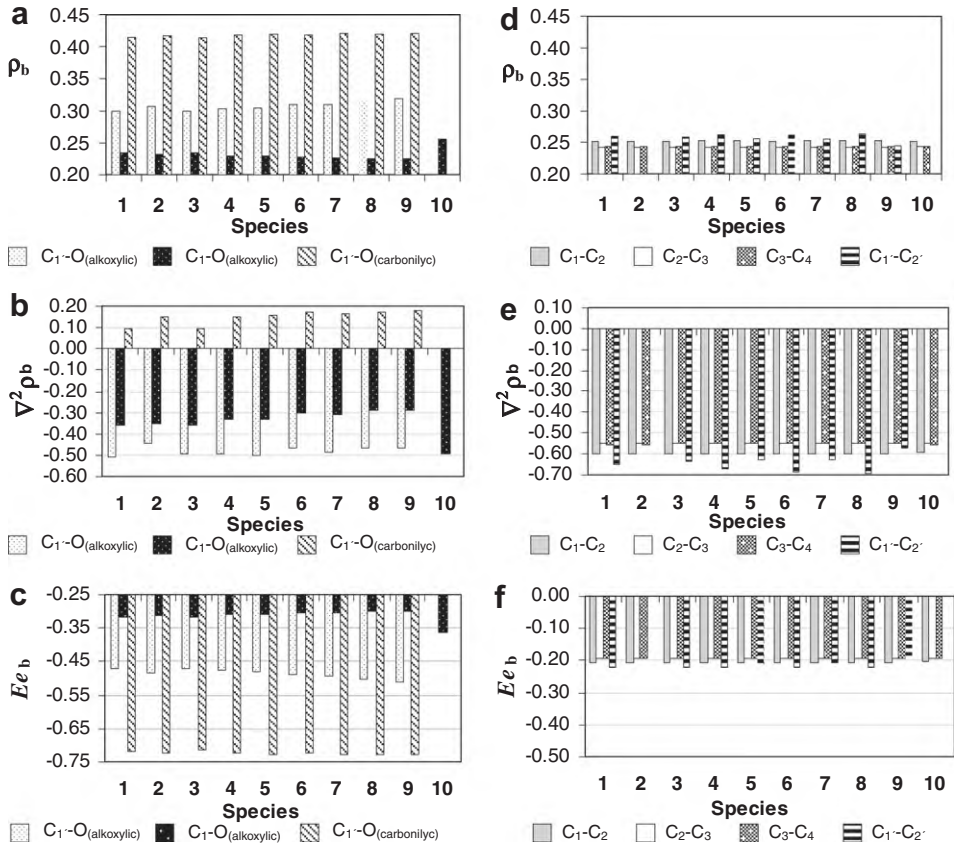

Figure 4. Local Topological properties of the electronic charge density calculated at the BCPs of selected bond paths for species **1**–**10**.

Likewise, it can be observed in Table 1 that in both alkoxylic C—O bonds the relationship G_b/ρ_b and the $E_{e(b)}$ values are lower in magnitude to the corresponding values in carbonylic C—O bond. It is also noticeable that the alkoxylic $C_{1'}$—O bond ellipticity is higher in **6**, **7**, **8**, and **9** analogues than in the natural sex pheromone. Similar effect can be seen in the carbonylic C—O bonds.

The topological properties at the BCP on $C_{1'}$—$C_{2'}$, C_1—C_2, C_2—C_3, and C_3—C_4 bonds are clearly indicative of shared interactions, namely a relatively large value for ρ_b and a negative value for $\nabla^2\rho_b$. Figure 4d and e shows the scarce variation of the charge density and $\nabla^2\rho_b$ in the different C—C bonds in relation to the C—O bonds. Slight changes on $C_{1'}$—$C_{2'}$ and even slighter on C_1—C_2 bond parameters can be observed due to the substitutions at $C_{2'}$. The charge density is around 0.25 au. and $\nabla^2\rho_b$ is negative in all cases. The relationship $|\lambda_1|/\lambda_3$ is appreciably greater than one; $E_{e(b)}$ is negative and show the same order of magnitude than ρ_b; and G_b/ρ_b is less than one (see Table 1). It is noticeable that, in those analogues substituted with fluorine, the ρ_b and $\nabla^2\rho_b$ values at the BCP on $C_{1'}$—$C_{2'}$ bond are slightly high, whether in analogues substituted with chlorine those values slightly decrease. Nevertheless, in all analogues the total energy density diminishes with relation to the natural sex pheromone. This means that these bonds undergo weak perturbations on the topology of the charge density. A deeper analysis has to be done and it will be described below.

3.1.2. Atomic properties

As it was mentioned at the beginning of this section, the third topological element to be considered between two atoms bonded together is the *interatomic surface* (IAS). The interatomic surface is defined by the set of trajectories of $\nabla\rho_{(r)}$ that terminate at a BCP. Accordingly, the Atoms in Molecules Theory defines an atom as a bounded portion of real space, known as atomic basin, and

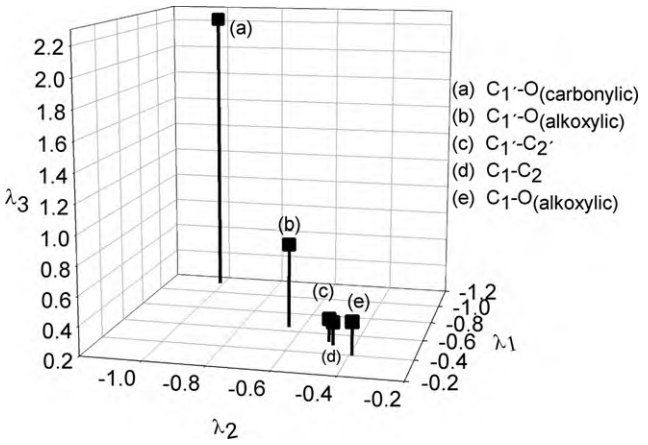

Figure 5. Vectors associated to the λ_{1-3} autovalues, at the BCP, for selected bonds in the sex pheromone.

is denoted by Ω. Therefore, all information about a particular AIM atom is contained in its finite volume and the properties can be obtained by integrating each corresponding density property over the atomic basin.[26,37] (see Fig. 6). The ability to determine the individual atomic contributions to the changes in population, charge, energy, and volume at a fragment (for example, in modified acetate group) should be of particular use for obtaining a better understanding of the subjacent modification produced in the analogues derivatives from the sex pheromone. In Figure 7 and Table 2, the atomic properties of selected atoms (corresponding to acetate/acetate modified group) from the natural sex pheromone (compound **1**) and analogues **2**–**10**, are shown. The atomic properties informed are the average number of electrons, $N_{(\Omega)}$, (from which the atomic net charge, $q_{(\Omega)}$, can be calculated as $Z_\Omega - N_{(\Omega)}$; being Z_Ω the nuclear charge of the atom); the atomic volume, $v_{(\Omega)}$, and the first moment of the atomic charge distribution, $|M_{(\Omega)}|$.

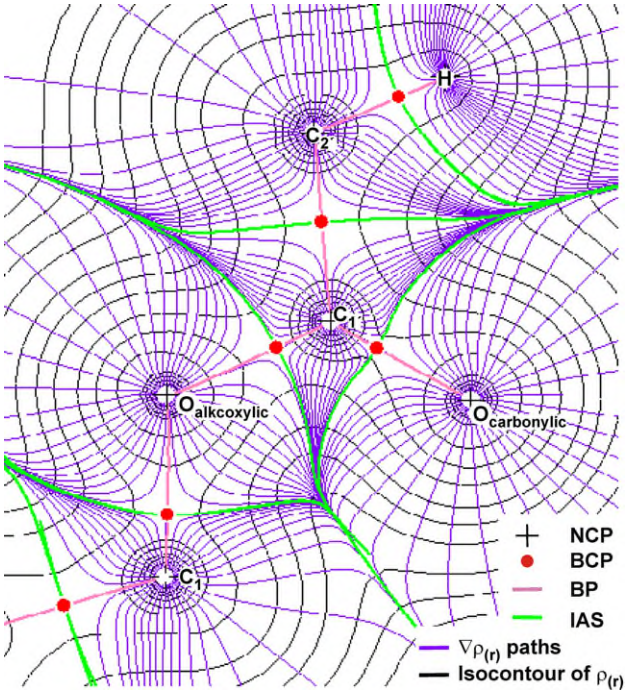

Figure 6. The bond paths, bond critical points, and interatomic surfaces superimposed on the electronic charge density isocontour lines in the molecular plane defined by O—$C_{1'}$(O)—$C_{2'}$ atoms, for compound **1**. The set of all gradient paths attracted to one nuclear critical point, (NCP), constitutes an atomic basin.

An analysis of our results shows that the atoms whose properties were significantly affected by substituents at $C_{2'}$ were the carbon and oxygen atoms at the acetate modified moiety. Subsequently, these modifications will be described separately in the following paragraphs.

3.1.2.1. Atomic properties modifications at the carbon atoms. Based upon the descriptors mentioned above, we can see in Figure 7a–c), that properties such as the electronic population and the volume at the $C_{2'}$, $C_{1'}$, and the C_1 atoms are noticeably different among them and that also show distinctions in the different surroundings. The evaluation of compounds **1**–**9** shows that some properties have a broader range of variation than others. The atomic carbon volumes vary in a range of 70 to 23 au. in $C_{2'}$ and of 45 to 32 au. in $C_{1'}$. This range of variation represents only 52 to 50 au. for the more distant C_1 carbon atom.

As it was mentioned above, the effect of the substitution of a hydrogen atom by electron withdrawing substituents (one, two, and three fluorine or chlorine atoms) is clearly reflected by the electronic population (or electronic charge) and the atomic volume. Undoubtedly, the larger decrease in both properties is observed upon the carbon atom where the substitution takes place ($C_{2'}$). This atom experiences a decrease in population and subsequent electronic destabilisation (due to a decrease of $-E_{(\Omega)}$, results not shown). The charge values upon $C_{2'}$ show strong variations from +0.072 in compound **1** (the natural sex pheromone) to +1.784 au. in analogue **8** (therefore this carbon atom is already 80 times more positive after the substitution of three hydrogen atoms by fluorine atoms). The volume has a decrease of about 26.6%, 48.2%, and 67.0% in compounds **4**, **6**, and **8** respectively compared to the natural sex pheromone. The IAS in the $C_{2'}$, in the direction of the substituents, also shows the major change in these compounds (results not shown). On the contrary, substitution of the H by CH_3 in analogue **3** at the $C_{2'}$ atom produces a low volume decrease of 16.0% (from 70.41 to 59.17 au.) as expected from the small differences in electronegativity between C and H atoms.

In the natural sex pheromone, the most electropositive carbon atom is the one bounded to both oxygen atoms, ($qC_{1'(\Omega)}$ = +1.593 au.) where, as well, the nucleophilic attack can occur (i.e., by interaction with a serine residue inside PBP). The replacement of hydrogen by halogen atoms at $C_{2'}$ produces a slight increase on the charge value on this atom ($qC_{1'(\Omega)}$ lie in the range between +1.593 to +1.731 au.). In contraposition, the charge upon C_1 atom diminish very slowly and the atomic volumes, the electronic energy and the dipolar polarizations do not show significant differences.

Figure 7 shows that the substituent's effects can be clearly seen by the atomic properties, such as population and volume, on the carbon atoms. Interestingly, the substituent's effects of the local properties at the BCP (charge density, Laplacian, and total electronic energy) are less visible than the atomic properties.

3.1.2.2. Atomic properties modifications at the oxygen atoms. In Figure 7d–f, the atomic properties ($N_{(\Omega)}$; $v_{(\Omega)}$, and $|M_{(\Omega)}|$, for carbonylic and alkoxylic oxygen atoms at acetate/modified acetate moieties in the sex pheromone and its analogues are shown. These results show that the properties assume higher values on the oxygen of the carbonyl group than on the oxygen of the alkoxyl group (for example the $|M_{(\Omega)}|$ in O(=C) is more than double in the carbonyl oxygen than in the alkoxyl oxygen). The electronic population of the oxygen atoms in carbonyl and alkoxyl groups decreases in the following order **1** ≈ **3** > **2** > **5** > **4** > **7** > **9** > **6** > **8**. It was, as well, observed that the oxygen atom of the carbonyl group is the most affected by the substitution of the H atom for

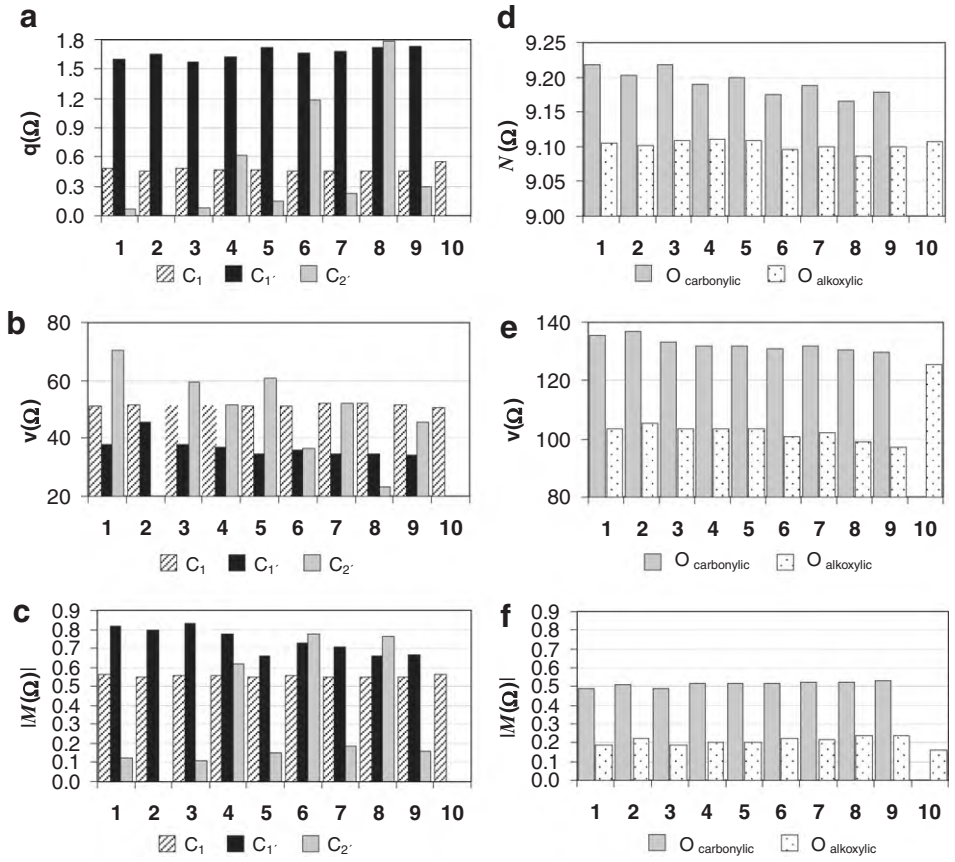

Figure 7. Atomic properties $q_{(\Omega)}$, $v_{(\Omega)}$, and $|M_{(\Omega)}|$ for selected carbon atoms (a–c); and $N_{(\Omega)}$, $v_{(\Omega)}$, and $|M_{(\Omega)}|$, for carbonylic and alkoxylic oxygen atoms (d–f), respectively; in the sex pheromone and its analogues.

Table 2
Atomic Properties of Selected Atoms in Species 1[a,b]

Atom	$N_{(\Omega)}$	$E_{(\Omega)}$	$v_{(\Omega)}$	$q_{(\Omega)}$	$\lvert M_{(\Omega)}\rvert$
$O_{(carbonylic)}$	9.218	−76.0547	135.26	−1.219	0.489
$O_{(alkoxylic)}$	9.105	−75.9864	103.44	−1.105	0.189
C_1	5.522	−37.7891	50.99	+0.478	0.562
$C_{1'}$	4.407	−37.0483	37.96	+1.593	0.818
$C_{2'}$	5.928	−38.0279	70.41	+0.072	0.120
$H_1(C_{2'})$	0.979	−0.6131	48.99	+0.021	0.134
$H_2(C_{2'})$	0.979	−0.6132	48.94	+0.021	0.134
$H_3(C_{2'})$	0.976	−0.6156	48.33	+0.024	0.133
$H_1(C_1)$	0.971	−0.6263	45.10	+0.028	0.138
$H_2(C_1)$	0.997	−0.6363	48.62	+0.003	0.139

[a] Atomic electron populations, $N_{(\Omega)}$; atomic energies, $E_{(\Omega)}$; atomic volume integrated to the 0.001 au isodensity envelope, $v_{(\Omega)}$; net atomic charge, $q_{(\Omega)}$, and atomic dipolar moment, $|M_{(\Omega)}|$ (all values in au.).
[b] 1 au (M) 8478 × 10^{-30} C m; 1 au. (E) 2.6255 kJ mol^{-1}.

electronegative atoms in $C_{2'}$. The variation of population upon alkoxylic oxygen is hardly noticeable.

The increase of the positive charge upon $C_{1'}$, (because of the electronegative atoms in the adjacent C atom) and the decrease of the negative charge upon the oxygen, both at the carbonyl group, (in the fluorinated **4**, **6**, and **8** analogues) are accompanied by a decrease in the dipolar moment upon the carbon atom and a light increase of the same property upon the carbonylic oxygen atom. In contrast to this result, and in accordance with what we expected, the substitution of the acetate group by a formate group (analogue **2**) or by a propionate group (analogue **3**), produces only a slight change in all the atomic properties examined. These results are in accordance to the biological response at the electroantennogram study where the reduction is only 17% in analogue **3** comparing to the activity of the natural sex pheromone that is 100%. The increase in volume by the addition of a methyl group is similar to the increase in volume by the addition of a chlorine atom. Therefore, the small diminish of the activity in analogue **3** should be attributed to the steric instead of the electronic effect.

The previous analysis indicates that the oxygen atoms achieve the decrease in the electronic population due to the extraction of electrons from the neighbouring carbon. In addition, fluorine and chlorine atoms behave in the same way. This results in the increase of the possibility of a nucleophilic attack at the $C_{1'}$ atom.

The decrease in the electronic population observed upon the two oxygen atoms was previously detected by MEPs. The MEPs indicated the decrease of negative electrostatic potential $V_{(r)}$ in fluorinated and chlorinated analogues. This was further confirmed and quantified by AIM analysis, as can be seen in Figure 7.

The successive replacement of hydrogen by fluorine atoms at the acetate moiety, results in the loss of electrons in the neighbouring atoms. Data shows that the values were: 0.542*e*, 1.106*e*, and 1.712*e* upon the carbon where the substitution took place; 0.034*e*, 0.073*e*, and 0.123*e* upon the carbonylic carbon; and 0.028*e*, 0.034*e*, and 0.053*e* upon carbonylic oxygen in **4**, **6**, and **8** analogues, respectively. It has also been observed that the loss of the electronic population on the carbon and oxygen atoms at the carbonyl group is lower in chlorinated than in fluorinated compounds. This tendency should be in accordance to the loss of the biological activity in halogenated compounds. Nevertheless, the biological activity is still lower in chlorinated analogues that in fluorinated analogues.

Even though the chlorine atom has a lower polarity than the fluorine atom, the chlorine atom is a more voluminous substituent; in consequence, the replacement of the hydrogen atoms in CH_3 group by Cl atoms raises the possibility of a steric hindrance. In compound **8** the CCl_3 group clearly occupies the largest area in the modified acetate moiety. Therefore, the oxygen atom of the alkoxyl group results scarcely accessible for intermolecular interactions. In conclusion, both electronic effect and steric hindrance may be deleterious to the biological activity.

An important observation is noticeable: in general, the similarity of the atomic volume of the fluorine and hydrogen atoms is accepted. However, our results show that the volume of the fluorine atom, calculated by AIM, is double that the volume of hydrogen, and half the volume of chlorine (i.e., $v_{(H)} = 48.99$ au. in **1**, $v_{(F)} = 108.75$ au. in **4**, and $v_{(Cl)} = 218.82$ au. in **5**). As a result, it is evident that the presence of a voluminous group in some analogues could impose an important steric hindrance and limit the perfect match with the PBP. Interestingly enough, the contraction of the carbon volume, ($C_{2'}$) is as well noticeable in these halogenated analogues.

3.2. Topology of the Laplacian of the charge density

The Laplacian of $\rho_{(r)}$ is an information-rich function. It should be distinguish that the topological description of the Laplacian of the electronic density distribution, $\nabla^2\rho_{(r)}$, is a powerful tool in the interpretation of quantum chemical results. It provides an enhanced view of the local form of the electronic density. We believe that a deep knowledge of the electronic structure of these analogues is essential in order to understand the mechanisms that occur during the recognition process in chemical communications of insects. For this reason, we describe, in the following paragraph, a study based on the topology of the Laplacian.

As it was mentioned at the beginning of the results section, the potential isosurface (Figure 2) shows that the region of attractive interaction localized on the modified acetate group undergoes larger changes when the hydrogen atom is substituted by electronegative atoms than when it is substituted by a methyl group. These graphs also show that the attractive region of the oxygen atom in the alkoxy group decreases in all cases. In addition, the attractive region near the carbonyl group always increases in the presence of electronegative atoms in the halo-acetate group.

More accurately, the topology of the Laplacian of the charge density can show in a molecular graph (with the localization of critical points in the tridimensional space), the localization of the preferential sites of attack between the nucleophiles, such as in the sex pheromone and its analogues, and the electrophiles such as in the PBP. In other words, a tridimensional chart can show whether the charge density is either maximally concentrated or maximally depleted. In the first case, (maximally concentrated charge) it is possible to report which sites are able to deliver electronic charge and, in consequence, that they are especially reactive toward electron-poor reactants (such as hydrogen atoms involved in hydrogen bonds). In the second case, it is possible to show which sites are able to stabilize an overload uptake of electronic charge and that they are especially reactive toward electron-rich reactants (i.e., oxygen atom at the serine residue).

In the natural sex pheromone, the oxygen atoms of the acetate group are sites that exhibit the highest concentration of charge. Therefore, it is assumed that from all the possible sites, the oxygen atoms will be the preferred ones for an electrophilic attack by the binding protein. Furthermore, it is essential to mention here that the electrophilic capacity of both oxygen atoms of the acetate group might be affected by the substitution of the hydrogen atom by fluorine or a chlorine atom. Moreover, it should also be taken into account that the presence of halogen atoms increases the number of possible sites of binding. Due to this fact, we consider that it will be interesting to explore the electronic effects of the substitution of the methyl hydrogen atoms of the acetate group by charge-withdrawing atoms such as F or Cl or by a donating —CH_3 group.

In this context, the AIM theory defines the valence–shell charge concentration (VSCC) as the outer region of an atom in one molecule where $\nabla^2\rho < 0$. The VSCC is of spherical symmetry in the isolated atom but it is distorted upon chemical combination, showing by this, a topology sensitive to different environments. The extremes or critical points in the distribution of the Laplacian function of ρ are classified by their rank and signature in the same way as it is done for the CPs in the charge density. The Laplacian CPs appear where $\nabla(\nabla^2\rho) = 0$ and the eigenvalues of the Hessian of $\nabla^2\rho$ indicate the principal curvatures of $\nabla^2\rho$ at the CP. In accordance with other authors,[23,27] it is convenient, for a more intuitive interpretation, to consider the $-\nabla^2\rho$ function for out studies. A (3, −3) CP corresponds to a local maximum (in a tridimensional chart) in $-\nabla^2\rho$ (with $\nabla^2\rho < 0$), and indicates a local electronic charge concentration (CC), while a (3, +3) CP corresponds to a local minimum in $-\nabla^2\rho$, (with $\nabla^2\rho > 0$) and indicates a local depletion of the electronic charge (CD).

3.2.1. Critical points of $-\nabla^2\rho$

Figure 8 shows the maxima CC points or (3, −3) critical points in $-\nabla^2\rho_{(r)}$, superimposed on the molecular graph (networks of bond path in the density topology). These points show the localizations of bonded and non-bonded maxima for the natural sex pheromone (**1**) and two tri-halogenated compounds (analogues **8** and **9**).

Table 3 shows the non-bonded maxima (nb) characterization of the VSCCs of oxygen, fluorine and chlorine atoms in the natural sex pheromone and its analogues.

It is important to emphasize that the existence of nonbonding maxima in the VSCC of the carbonyl and alkoxyl oxygen atoms as well as chlorine and fluorine in halo-acetate groups, indicates

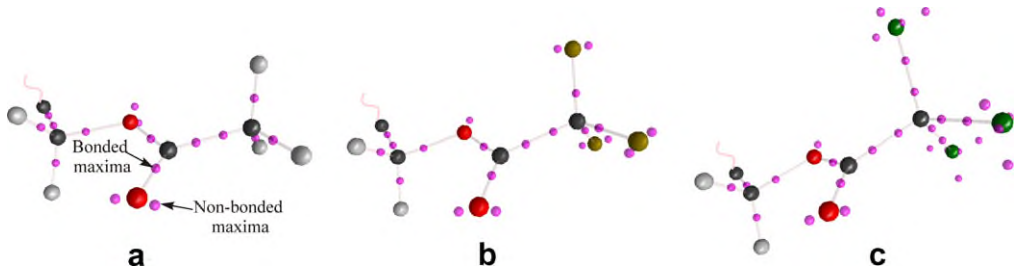

Figure 8. Critical points of the $-\nabla^2\rho$ distribution superimposed on molecular graph in acetate/halo-acetate function for species (a) sex pheromone, (b) analogue **8**, and (c) analogue **9**. In all cases, note the two maximum bonded in the VSCC of the carbon atoms, along of the C—C bond. In (b) it can be noted one b-CP along of the C—F bonds and in (c) two b-CPs along of the C-Cl bonds. Note the localization of the nb-CPs on carbonylic and alkoxylic oxygen atoms and fluorine and chlorine atoms.

Table 3
Characterization of non-bonded máxima for the VSCCs for oxygen, fluorine and chlorine atoms by B3LYP/6-31++G** in 1-10 compounds.

Atom	Compound	Non-bonded maxima (nb)			
			#nb	$\nabla^2\rho_{(r)}$[a]	r (au.)[a]
$O_{carbonylic}$	1		2	6.138	0.634
	2		2	6.095	0.635
	3		2	6.141	0.634
	4		2	5.973	0.636
	5		2	6.149	0.634
	6		2	6.162	0.634
	7		2	6.102	0.634
	8		2	6.179	0.634
	9		2	6.130	0.634
	10		—	—	—
$O_{alkoxylic}$	1		2	5.824	0.637
	2		1	5.853	0.637
	3		2	5.821	0.637
	4		1	5.953	0.635
	5		1	5.926	0.636
	6		1	5.871	0.636
	7		1	5.867	0.636
	8		1	5.921	0.636
	9		1	5.931	0.636
	10		2	6.546	0.632
F	4	F_1	2	11.742	0.553
	6	F_1	2	11.888	0.553
		F_2	2	11.853	0.553
	8	F_1	2	11.627	0.554
		F_2	2	11.676	0.553
		F_3	2	11.613	0.554
Cl	5	Cl_1	3	0.834	1.168
	7	Cl_1	2	0.849	1.166
		Cl_2	2	0.841	1.167
	9	Cl_1	3	0.844	1.166
		Cl_2	3	0.854	1.166
		Cl_3	3	0.844	1.166

[a] When the number of the non-bonded maxima (#nb) is $\neq 1$ the average value of the properties is given.

new sites for electrophilic attract and H bonding in these molecules.

As it is well known, the fluorine atom is the most compact, from all analyzed atoms, and presents the smallest radius of the non bonded maxima. It also shows the highest value of the negative $-\nabla^2\rho_{(r)}$ (approximately 11.7 au.). This represents almost twice as much as the $-\nabla^2\rho_{(r)}$ values of the O atom. (Oxygen possesses the second the highest value around of 5.8–6.5 au.). As it is expected in the third period of the periodic table, the Cl atom shows the lowest values of the $-\nabla^2\rho_{(r)}$ and the highest distance from non-bonded critical point (nb-CP) in valence shell at the nucleus.

3.2.2. Oxygen VSCC

In the carbonyl oxygen atoms, at the acetate or the modified acetate moieties in the sex pheromone or its analogue derivatives respectively, two nonbonding charge concentrations, corresponding to the classical 'lone pairs' in the carbonyl oxygen VS, were found (Table 3). Such non-bonding charge concentrations have been shown to be the sites for either protonation or H-bonding.[37] Both of them will be discussed below. The position of every maxima in these O atoms is not symmetrically located at 120 degrees from the C=O bond direction in the molecules we studied here. If a non-symmetrical environment is present in the immediate vicinity of the carbonyl group, like in the halo-acetate group, then its maxima will be located in non-symmetrical positions in the oxygen VS. This shows the influence of the electric field produced by electron withdrawing substituents ('neighbouring' atoms) in the position of the VSCC maxima of the carbonyl oxygen atom (Table 2).

Moreover, this substitution effect at the 'neighbouring' carbon atoms is observed upon the alkoxyl oxygen atom in halogenated analogues. In the alkoxyl oxygen atom, two non-bonding charge concentrations were found in the sex pheromone and in analogue **3**, where a methyl group was replaced by an electron donating ethyl group.

The position of the CP of maxima VSCC is located, above and below the plane that contains the C_1—O—$C_{1'}$ nuclei and exhibits similar values in terms of distances to the nucleus and $-\nabla^2\rho_{(r)}$. In addition, two nb-CPs at the oxygen valence shell were found in the alcohol analogue, (compound **10**) with values that were slightly higher than the previous ones.

The presence of electron withdrawing substituents, such as fluorine and chlorine, modifies the topology of the Laplacian at the oxygen valence shell. In these cases (analogues **4**–**9**) only one non-bonding maxima appears in the oxygen valence shell. Its localization is at the middle of the two now missing critical point and it is positioned in the same plane as the C_1—O—$C_{1'}$ fragment.

3.2.3. Chlorine and Fluorine VSCCs

The chlorinated compounds exhibit three (3, −3) nb-CPs at the chlorine VS, and show a tetrahedral form for this maxima. This is in consistence with the valence shell electron pair repulsion (VSEPR) model. Two bonded critical points (b-CPs) in the C—Cl bond direction were found: one (3, −3) b-CP at the chlorine VS and another one at the carbon VS. In contrast, the valence shell of F atoms revealed only two non-bonded maxima in the studied analogues (Fig. 8b and c). In general, the bonding of a F with a C atom is such that it forms a single bond (showed only one b-CP between both atoms) with three non-bonding maxima localized[38] in its VSCC, such as in the CH_3F case. If the negative hyperconjugation is present, this effect will create a partial double bond character in the F—C bonds. In this situation, only two 'lone pairs' will be present in the fluorine VS as non-bonding maxima of CC. They will be located in the molecular plane and approximately 120–140 degrees from the F—C bond direction. In addition, when conjugation is present, an increase in the density (especially in the bond ellipticity) is expected to occur at the BCP with respect to those of a single F—C bond. The latter seems to be the case of the fluorine atoms in analogues **4**, **6**, and **8** (Table 3).

In summary, the results in Table 3 show that one site (corresponding to one nb-CP at alkoxyl oxygen atom VS) disappears and six new sites appear in the trifluorinated compound.

As it has been previously described, the Laplacian of the electronic charge density can be used as an indicator of protonation sites of a molecule.[37] This may be of great help in the pheromone field. Popelier et al.[39] have investigated and discussed to what extent the function evaluated at the nb-CP of CC in the atomic VS can be used as an indicator of protonation energy. These authors have emphasized that an essential condition for the success of the Laplacian is that the protonation trends should be established in a series where the local environment of the protonation site is not too perturbed. In other words, although this function correctly predicts the protonation site in substituted aldehydes, the Laplacian values cannot be used in a comparative form over atoms with different atomic numbers (i.e., oxygen, fluorine, and chlorine) to predict the preferred site of protonation.

In consequence, we would like to emphasize that in the analogues we studied the highest values of $-\nabla^2\rho_{(r)}$ in fluorine atoms should not be interpreted as of the highest susceptibly to electrophilic attack. In concordance to what we mention above, Grabowski[40] has established that, although the fluorine atom is the more electronegative atom in the periodic table, it is also a weak proton acceptor and that this property decreases by the addition of another fluorine atom.

In the same way the regions of charge depletion, (3, +1) CP, in the VSCC of the C atom, have been identified as sites of nucleophilic attack in methanal and similar compounds.[27,41] Therefore, it is evident that the carbonyl groups in our set of analogues are candidates for such type of attack and that the carbonyl carbon atoms with the largest depletion in their VSCC will be the most susceptible to nucleophilic attack.[41,42] Subsequently, the carbonylic carbon atoms in halogenated analogues (analogues **4**–**9**) showed an increase capability for such attack because they have a greater region of charge depletion in their VSCC to be filled (data not shown). These results are consistent with the observation of the decrease of the electronic population and the increase of positive charge in $C_{1'}$ (Fig. 7).

4. Conclusions

A theoretical study of the electronic properties of the sex pheromone and its analogue derivatives in the female processionary moth *T. pytiocampa* is accomplished in this work within the framework of the density functional theory. Using the Bader's quantum topological theory of atoms in molecules as well as the molecular electrostatic potential analysis on the van der Waals surface, we were able to rationalize the effect of the substitution of hydrogen atoms in the acetate group on the electronic charge density distribution.

Based in the electrostatic potential analysis on the molecular surface, a remarkable result of this work shows that, in addition to the oxygen atoms of the acetate group or modified acetate in the compounds studied here, the electrophilic region defined by the enyne group is a site that exhibit a very high (but not the highest) concentration of electronic charge density. In consequence, the distance between both sites might be considered as an indicator of the electronic requirement in the molecular recognition process.

As a result of the electron withdrawing effect, the substitution of hydrogen atoms by halogen atoms produce a diminish of the electronic population in the oxygen and carbon atoms at the carbonyl group. This may explain the diminish of the capacity of the oxygen atoms as hydrogen acceptor, in the modified ester moiety of the pheromone analogues. These results reinforce the idea that the crucial interaction between the acetate group of the pheromone and the receptor PBP is most likely a hydrogen bonding that is affected by the substitution of atoms at this group.

In addition, the replacement of an H atom by an electron donor substituent, such as the methyl group, or in other words, the replacement of a methyl group by an ethyl group in the ester function, produces only a small electronic change and a major steric effect with a scarce reduction in the pheromonal activity.

The variation in the atomic properties, such as electronic population and atomic volume, are sensitive identifiers of the loss of the biological activity in the analogues studied here. Additionally, the modified acetate group, with electronegative atoms, shows new charge concentration critical points or regions of charge density concentration in which an electrophilic attack can occur as well.

Finally, the use of the topological analysis, (based in the charge density distribution and its Laplacian function), in conjunction with MEPs, provide valuable information about the steric volume and electronic requirement of the natural sex pheromone in its interaction with the PBP. In addition, a deep electronic analysis of other analogues and the potential interactions with the PBP are under investigation in our laboratory and the results will be published in the near future.

Acknowledgments

The authors acknowledge to the CONICET, Argentine for Grant PIP 6337 and to SECYT UNNE and SECYT UTN-FRRe for financial support. M.F.Z. is a fellow of CONICET and N.M.P. is career researcher of CONICET, Argentine.

References and notes

1. Anderson, P.; Hansson, B. S.; Nilsson, U.; Ha, Q.; Sjöholm, M.; Skals, N.; Anton, S. *Chem. Senses* **2007**, *32*, 483–491.
2. Tregoni, M.; Campanacci, V.; Cambellau, C. *Trends Biochem. Sci.* **2004**, *29*, 257–264. and references therein.
3. Baker, T. C.; Ochieng', S. A.; Cossé, A. A.; Lee, S. G.; Todd, J. L.; Quero, C.; Vickers, N. *J. Comput. Physiol. A* **2004**, *190*, 155–165.
4. Rosell, A.; Guerrero, G. *Curr. Med. Chem.* **2005**, *12–14*, 461–469.
5. (a)*Behaviour-Modifying Chemical for Insect Management*; Ridgway, R. L., Silverstein, R. M., Inscoe, M. N., Eds.; Marcel Dekker, Inc.: New York, 1990; (b) Renou, M.; Guerrero, A. *Annu. Rev. Entomol.* **2000**, *45*, 605–630.
6. Pelosi, P. *J. Neurobiol.* **1996**, *30*, 3–19.
7. *Nucleosides and Nucleotides as Antitumor and Antiviral Agents*; Chu, C. K., Baker, D. C., Eds.; Plenum Press: New York, 1993.
8. Camps, F.; Coll, J.; Guerrero, A.; Riba, M. *J. Chem. Ecol.* **1983**, *9*, 869–875.
9. Camps, F.; Fabrias, G.; Gasol, V.; Guerrero, A.; Hernandez, R.; Montoya, R. *J. Chem. Ecol.* **1988**, *14*, 1331–1346. and references therein.
10. Guerrero, A.; Murgó, R.; Martorell, X. *Physiol. Entomol.* **1986**, *11*, 73–77.
11. Quero, C.; Camps, F.; Guerrero, A. *J. Chem. Ecol.* **1995**, *21*, 1957–1969.
12. Parrilla, A.; Guerrero, A. *Chem. Senses* **1994**, *19*, 1–10.
13. (a) Camps, F.; Gasol, V.; Guerrero, A. *J. Chem. Ecol.* **1990**, *16*, 1155–1172; (b) Renou, M.; Berthier, A.; Guerrero, A. *Pest Manag. Sci.* **2002**, *58*, 839–844.
14. Feixas, J.; Prestwich, G. D.; Guerrero, A. *Eur. J. Biochem.* **1995**, *234*, 521–526.
15. Bau, J.; Martinez, D.; Renou, D.; Guerrero, A. *Chem. Senses* **1999**, *24*, 473–480.
16. Parrilla, A.; Villuendas, I.; Guerrero, A. *Bioorg. Med. Chem.* **1994**, *8*, 845.
17. Ashour, M-B. A.; Hammock, B. D. *Biochem. Pharmacol.* **1987**, *36*, 1869–1879.
18. Prestwich, G. D.; Streinz, L. *J. Chem. Ecol.* **1988**, *14*, 1003–1021.
19. (a) Politzer, P.; Truhlar, D. G. *Chemical Applications of Atomic and Molecular Electrostatic Potentials*; Plenum Publishing: New York, 1991; (b) Ruiz, J.; Perez, C.; Pouplana, R. *Bioorg. Med. Chem.* **2003**, *11*, 4207–4216; (c) Boer, D. R.; Kooijman, H.; Van der Louw, J.; Groen, M.; Kelder, J.; Kroon, J. *Bioorg. Med. Chem.* **2001**, *9*, 2653–2659.
20. Okulik, N.; Jubert, A. *J. Mol. Struct. (THEOCHEM)* **2006**, *769*, 135–141.
21. Greeling, P.; Langenaeker, W.; De Proft, F.; Baeten, A.. In *Molecular Electrostatic Potentials: Concepts and Applications. Theoretical and Computational Chemistry*; Elsevier Science B.V.: Amsterdam, 1996; vol. 3, pp 587–617.
22. Leach, A. R. In *Molecular Modelling: Principles and Applications*, 2nd ed.; Pearson Education: EMA, 2001.
23. Lobayan, R. M.; Sosa, G. L.; Jubert, A. H.; Peruchena, N. M. *J. Phys. Chem. A* **2005**, *109*, 181.
24. Matta, C. F.; Boyd, R. J. In *Quantum Theory of Atoms in Molecules: From Solid State to DNA and Drug Design*; Wiley-VCH: Weinheim, Germany, 2007.
25. Koritsanszky, T.; Flaig, R.; Zobel, D.; Krane, H. G.; Morgenroth, W.; Luger, P. *Science* **1998**, *279*, 356.
26. Bader, R. F. W. In *Atoms in Molecules. A Quantum Theory*; Oxford Science Publications, Clarendon Press: London, 1990.
27. Popelier, P. L. A. In *Atoms in Molecules. An Introduction*; Pearson Education: Harlow, UK, 2000.
28. (a) Becke, A. D. *J. Chem. Phys.* **1993**, *98*, 5648; (b) Lee, C.; Yang, W.; Parr, R. G. *Phys. Rev. B* **1988**, *37*, 785.
29. Frisch, M. J.; Trucks, G. W.; Schlegel, H. B.; Scuseria, G. E.; Robb, M. A.; Cheeseman, J. R.; Montgomery, J. A.; Jr., T.V.; Kudin, K. N.; Burant, J. C.; Millam, J. M.; Iyengar, S. S.; Tomasi, J.; Barone, V.; Mennucci, B.; Cossi, M.; Scalmani, G.; Rega, N.; Petersson, G. A.; Nakatsuji, H.; Hada, M.; Ehara, M.; Toyota, K.; Fukuda, R.; Hasegawa, J.; Ishida, M.; Nakajima, T.; Honda, Y.; Kitao, O.; Nakai, H.; Klene, M.; Li, X.; Knox, J. E.; Hratchian, H. P.; Cross, J. B.; Adamo, C.; Jaramillo, J.; Gomperts, R.; Stratmann, R. E.; Yazyev, O.; Austin, A.J.; Cammi, R.; Pomelli, C.; Ochterski, J. W.; Ayala, P. Y.; Morokuma, K.; Voth, G. A.; Salvador, P.; Dannenberg, J. J.; Zakrzewski, G.; Dapprich, S.; Daniels, A. D.; Strain, M. C.; Farkas, O.; Malick, D. K.; Rabuck, A. D.; Raghavachari, K.; Foresman, J. B.; Ortiz, J. V.; Cui, Q.; Baboul, A. G.; Clifford, S.; Cioslowski, J.; Stefanov, B. B.; Liu, G.; Liashenko, A.; Piskorz, P.; Komaromi, I.; Martin, R. L.; Fox, D. J.; Keith, T.; Al-Laham, M. A.; Peng, C. Y.; Nanayakkara, A.; Challacombe, M.; Gill, P. M. W.; Johnson, B.; Chen, W.; Wong, M. W.; Gonzalez, C.; Pople, J. A. Gaussian 03, Revision D.01; Gaussian, Inc.: Wallingford, CT, 2004.
30. Schlegel, H. B. *J. Comput. Chem.* **1982**, *3*, 214.
31. MOLEKEL 4.3, Flúkiger, P.; Lúthi, H.P.; Portmann, S.; Weber, J. Swiss Center for Scientific Computing, Manno (Switzerland), 2000.
32. *AIMPAC*: a suite of programs for the theory of atoms in molecules; Bader, R. F. W., co-workers, Eds.; McMaster University: Hamilton, Ontario, Canada.
33. Blieger-König, F.; Schönbohn, J. *AIM2000* Program Package, Version. 2.0 Copyright **2002.** Chemical adviser by Bader, R.F.W.; McMaster University. Hamilton, Canadá.
34. Blieger-König, F.; Bader, R. F. W.; Tang, T. H. *J. Comput. Chem.* **1982**, *3*, 317.
35. Popelier, P. L. A.; Smith, P. J. *Eur. J. Med. Chem.* **2006**, *41*, 862–873.
36. Cremer, D.; Kraka, E. *Croat. Chem. Acta* **1984**, *57*, 1259.
37. Carroll, M. T.; Chang, C.; Bader, R. F. W. *Mol. Phys.* **1988**, *63*, 387–405.
38. Castillo, N.; Boyd, R. J. *Chem. Phys. Lett.* **2005**, *403*, 47.
39. Popelier, P. L. A.; Smith, P. J. *Phys. Chem. Chem. Phys.* **2001**, *3*, 4208–4212.
40. Checinska, L.; Grabowski, S. J. *Chem. Phys.* **2006**, *327*, 202–208.
41. Carroll, M. T.; Cheeseman, J. R.; Osman, R.; Weinstein, H. *J. Phys. Chem.* **1989**, *93*, 5120–5123.
42. Murgich, J.; Franco, H. J.; San-Blas, G. *J. Phys. Chem. A* **2006**, *110*, 10106–10115.

View publication stats